© 2021. Published by The Company of Biologists Ltd | Journal of Cell Science (2021) 134, jcs253682. doi:10.1242/jcs.253682

RESEARCH ARTICLE

Vacuolar protein Tag1 and Atg1–Atg13 regulate autophagy termination during persistent starvation in *S. cerevisiae*

Shintaro Kira[1], Masafumi Noguchi[2,3], Yasuhiro Araki[1], Yu Oikawa[4], Tamotsu Yoshimori[3,5], Aiko Miyahara[2,5] and Takeshi Noda[1,2,*]

ABSTRACT

Under starvation conditions, cells degrade their own components via autophagy in order to provide sufficient nutrients to ensure their survival. However, even if starvation persists, the cell is not completely degraded through autophagy, implying the existence of some kind of termination mechanism. In the yeast *Saccharomyces cerevisiae*, autophagy is terminated after 10–12 h of nitrogen starvation. In this study, we found that termination is mediated by re-phosphorylation of Atg13 by the Atg1 protein kinase, which is also affected by PP2C phosphatases, and the eventual dispersion of the pre-autophagosomal structure, also known as the phagophore assembly site (PAS). In a genetic screen, we identified an uncharacterized vacuolar membrane protein, Tag1, as a factor responsible for the termination of autophagy. Re-phosphorylation of Atg13 and eventual PAS dispersal were defective in the *Δtag1* mutant. The vacuolar luminal domain of Tag1 and autophagic progression are important for the behaviors of Tag1. Together, our findings reveal the mechanism and factors responsible for termination of autophagy in yeast.

KEY WORDS: Tag1, Atg1, Atg13, PP2C phosphatase, Microautophagy, Autophagy, Yeast

INTRODUCTION

Macroautophagy (hereafter, autophagy) is a degradation process in which targets are enwrapped by autophagosomes and eventually degraded in the lysosome or vacuole (Mizushima and Komatsu, 2011). Autophagosome formation is executed by a group of Atg proteins, and the mechanism of autophagic progression have been studied intensively for several decades. Triggering autophagy by a stimulus such as nitrogen starvation leads to a series of events that includes phosphorylation of Atg proteins and their recruitment to sites of autophagosome formation (Reggiori and Klionsky, 2013). An important question is whether and how autophagy is terminated. Because autophagy is a self-degradation process, failure to properly terminate autophagy can ultimately lead to cell death (Kroemer and Levine, 2008). Although autophagic cell death is a recognized form of regulated cell death, most autophagy is related to pro-survival processes, suggesting the existence of mechanisms that terminate autophagy at appropriate points. In mammalian cells, autophagy terminates under persistent starvation (Yu et al., 2010). Specifically, ubiquitin-dependent degradation of Ulk1 and Vps34 (also known as PIK3C3) is responsible for termination of autophagy (Liu et al., 2016). In NRK cells, TORC1 is inactivated under serum starvation but eventually re-activated under further serum starvation, leading to termination of autophagy (Yu et al., 2010). Nevertheless, the termination mechanism remains to be elucidated.

In this study, we examined the mechanisms underlying termination of autophagy in the yeast *Saccharomyces cerevisiae*, and found that Atg1–Atg13 plays an important role in this phenomenon. Furthermore, we identified a novel vacuolar membrane protein, Tag1, that is responsible for this process.

RESULTS

Autophagy terminates after 10 h of nitrogen starvation in yeast

We first followed the autophagic activity of yeast cells under nitrogen-deficient conditions. We measured autophagic activity by means of an alkaline phosphatase (ALP) assay in strains bearing genomic integrations of Pho8Δ60, a vacuolar alkaline phosphatase genetically engineered to be expressed in the cytosol (Araki et al., 2017). In these cells, ALP activity reflects the integrative amount of cytosol transported into the vacuole after onset of autophagy (Araki et al., 2017; Noda et al., 1995). Within 1 h of shifting to a nitrogen starvation medium from a nutrient-rich medium (YEPD), ALP activity increased steeply and was sustained for 2–4 h (Fig. 1A). From 4 to 8 h after the shift, the sustained increase in ALP activity started to decrease, and ultimately stopped around 10 h, whereas the expression level of the Pho8Δ60 protein was maintained until 24 h of starvation (Fig. 1A; Fig. S1A). These observations indicate that autophagy is terminated 8–10 h after a shift to nitrogen starvation conditions, implying the existence of some molecular mechanism responsible for this process.

Autophagy termination in yeast is not mediated by TORC1

We asked whether TORC1, the master regulator of autophagy, is involved in autophagy termination (Noda, 2017). Sch9 is phosphorylated at S737 by TORC1. Hence, we monitored TORC1 activity by western blotting using the anti-Sch9 phospho-S737 antibody (Urban et al., 2007). In wild-type cells, the phosphorylated form of Sch9 was observed in nutrient-rich conditions, but disappeared after 0.5–2 h of starvation (Fig. 1B). Sch9 was re-phosphorylated after 12–24 h of starvation (Fig. 1B). In the autophagy-defective *Δatg2* mutant, however, re-phosphorylation of Sch9 was significantly reduced after 24 h of starvation (Fig. 1B). Treatment with rapamycin compromised the re-phosphorylation of Sch9 (Fig. 1B). Thus, in yeast, as in mammalian cells, TORC1 is

[1]Center for Frontier Oral Science, Graduate School of Dentistry, Osaka University, Yamadaoka 1-8, Suita, Osaka 565-0871, Japan. [2]Department of Oral Frontier Biology, Graduate School of Frontier Biosciences, Osaka University, Yamadaoka 1-8, Suita, Osaka 565-0871, Japan. [3]Laboratory of Intracellular Membrane Dynamics, Graduate School of Frontier Biosciences, Osaka University, Yamadaoka 2-2, Suita, Osaka 565-0871, Japan. [4]Research Center of Cell Biology, Institute of Innovative Research, Tokyo Institute of Technology, Nagatsuta 4259, Yokohama, Kanagawa 226-8503, Japan. [5]Department of Genetics, Graduate School of Medicine, Osaka University, Yamadaoka 2-2, Suita, Osaka 565-0871, Japan.

*Author for correspondence (takenoda@dent.osaka-u.ac.jp)

M.N., 0000-0002-9702-2171; A.M., 0000-0003-4816-1973; T.N., 0000-0003-3581-7961

Handling Editor: Jennifer Lippincott-Schwartz
Received 2 September 2020; Accepted 19 January 2021

Journal of Cell Science (2021) 134, jcs253682. doi:10.1242/jcs.253682

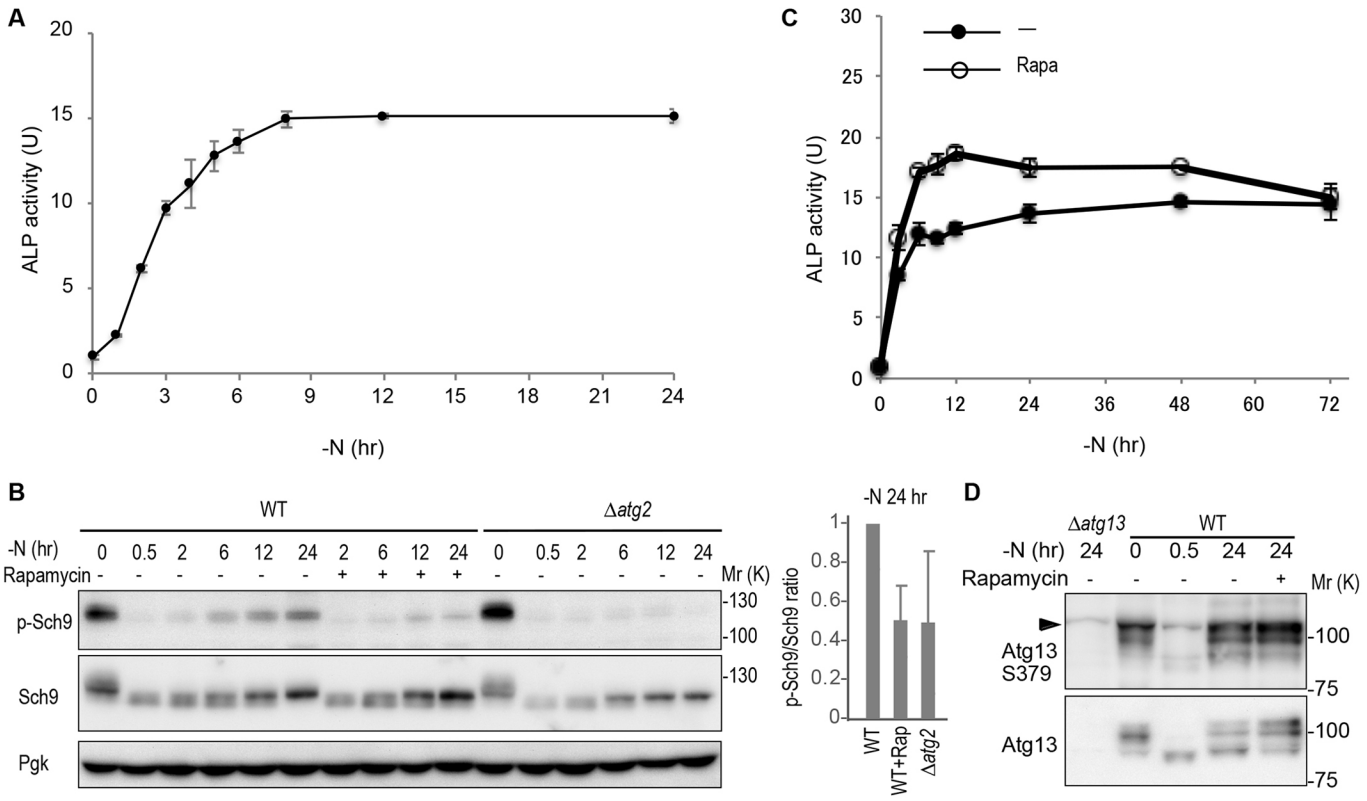

Fig. 1. Autophagy in yeast is terminated under persistent nitrogen starvation independently of TORC1. (A) Wild-type (WT; TNY509) cells were incubated in SD-N (pH 6.2) and subjected to an ALP assay at the indicated time points over 24 h (n=3). (B) Wild-type (BY4741) and Δ*atg2* (YKOL1970) cells were starved for 0, 0.5, 2, 6, 12, and 24 h with or without rapamycin and subjected to western blot analysis with anti-Sch9 and anti-phospho T737 Sch9 antibodies. Ratio of p-Sch9 and Sch9 band intensities in 24-h-starved samples were normalized against Pgk, and are represented by relative values (n=3). (C) WT (TNY509) cells were cultured in SD-N (pH 6.2) with or without 0.2 µg/ml rapamycin for the indicated times and subjected to the ALP assay (n=3). (D) Wild-type (BY4741) andΔ *atg13* (YKOL5600) cells were starved for 0, 0.5 or 24 h, with or without rapamycin, and subjected to western blot analysis with anti-Atg13 and anti-phospho-S379 Atg13 antibodies. A representative blot of two independent experiments is shown. Arrowhead indicates a non-specific band. Quantitative results are shown as mean±s.d.

re-activated under persistent starvation in a manner dependent upon autophagy (Yu et al., 2010).

If autophagy termination were dependent on TORC1 re-activation, inhibition of TORC1 activity would cause a defect in this process. However, when cells were cultured in nitrogen-deficient medium in the presence of rapamycin, autophagy termination was not affected (Fig. 1C). Reactivation of TORC1 has been proposed to be regulated by Gtr2, which in its GTP-bound form directly binds to TORC1 and inactivates it (Kira et al., 2014; Péli-Gulli et al., 2015). Conversion of Gtr2 from its GTP-bound form to the GDP-bound form is catalyzed by the GTPase-activating protein (GAP) Lst4–Lst7 heterodimer, the counterpart of mammalian folliculin–FNIP (Péli-Gulli et al., 2015; Petit et al., 2013; Tsun et al., 2013). However, autophagy terminated normally in Δ*lst7* cells, suggesting that TORC1 reactivation via Gtr2 does not play an important role in autophagy termination (Fig. S1B).

Next, we monitored Atg13, which is directly phosphorylated by TORC1 under nutrient-rich conditions and promptly dephosphorylated under nitrogen starvation to induce autophagy (Kamada et al., 2000). When nitrogen starvation is extended to 12 h, it is re-phosphorylated (Shin and Huh, 2011) (Fig. 1D). In addition, we monitored Atg13 phosphorylation status over a time course; re-phosphorylation of Atg13 started gradually after 8–10 h starvation (Fig. S1C), which correlates with the timing of autophagy termination (Fig. 1A). We asked whether this re-phosphorylation was mediated by TORC1 kinase. To address this issue, we first starved cells for 30 min, after which Atg13 was completely dephosphorylated. The cells were then cultured under starvation conditions with or without rapamycin for an additional 24 h. Atg13 was re-phosphorylated even in the presence of rapamycin (Fig. 1D). To inactivate TORC1 kinase activity in another way, we utilized *Gtr1* and *Pib2* mutants, which are upstream regulators of TORC1 (Kim and Cunningham, 2015; Michel et al., 2017; Tanigawa and Maeda, 2017; Ukai et al., 2018; Varlakhanova et al., 2017). To ablate both genes without killing the cells, as the double deletion mutant is lethal, *GTR1* was deleted and Pib2 expression was conditionally suppressed through the addition of doxycycline using the TETO7^{off} promoter system with degron (Gnanasundram and Koš, 2015), which inactivates TORC1 and arrests growth (Ukai et al., 2018). Although Pib2 protein levels were reduced in the absence of doxycycline-induced suppression after 24 h of starvation, doxycycline treatment further decreased the level of Pib2 (Fig. S1D). In this strain, TORC1 reactivation was suppressed in the presence or absence of doxycycline, but Atg13 was still re-phosphorylated at 24 h (Fig. S1D). These data indicate that Atg13 re-phosphorylation is not mediated by TORC1 kinase and that autophagy termination is not dependent on TORC1 re-activation.

Atg1 kinase is responsible for Atg13 re-phosphorylation in persistent starvation

We next asked which kinase is responsible for re-phosphorylation of Atg13 under persistent starvation. Atg1 is a protein kinase that interacts with Atg13 (Kamada et al., 2000; Yamamoto et al., 2016).

Journal of Cell Science (2021) 134, jcs253682. doi:10.1242/jcs.253682

Atg13 re-phosphorylation did not occur in Δ*atg1* cells, reproducing results from a previous report (Shin and Huh, 2011) (Fig. 2A), raising the possibility that autophagy is required. However, normal Atg13 re-phosphorylation was observed in Δ*atg2* cells, which is also defective in autophagy (Fig. 2A). Furthermore, in Δ*atg1* Δ*atg2* double deletion mutants, Atg13 was not re-phosphorylated (Fig. 2A). In Δ*atg17* cells, Atg13 phosphorylation was defective, implying that the integrity of the Atg1 complex is important for re-phosphorylation (Fig. S2A). Deletion mutants of other core components of the Atg machinery, Δ*atg3*, Δ*atg9*, Δ*atg14* and Δatg*18*, did not exhibit a defect

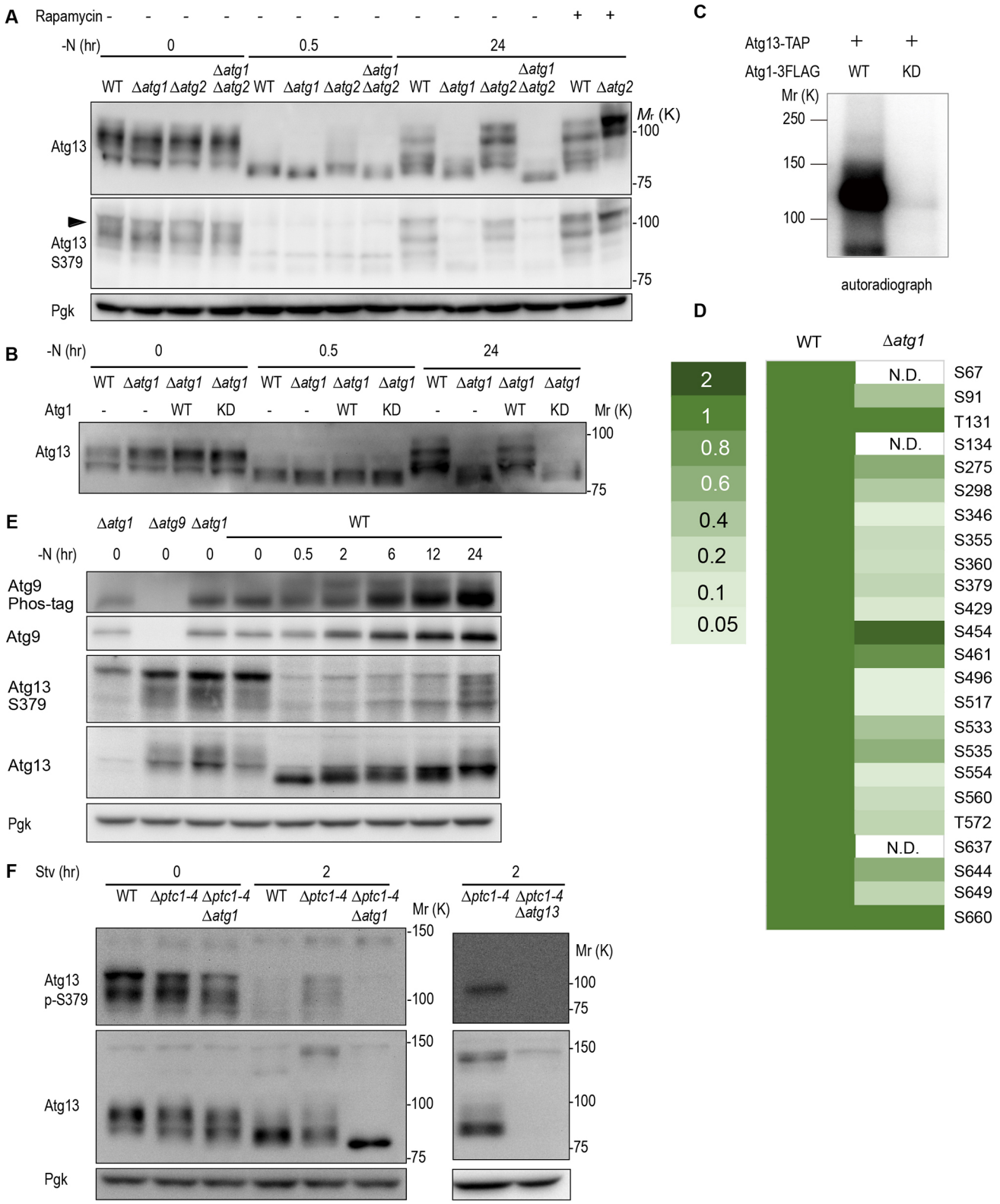

Fig. 2. See next page for legend.

Journal of Cell Science (2021) 134, jcs253682. doi:10.1242/jcs.253682

Fig. 2. Atg1 kinase re-phosphorylates Atg13 in persistent starvation. (A) Wild-type (WT; BY4741), Δ*atg1* (YKOL7090), Δ*atg2* (YKOL1970) and Δ*atg1*Δ*atg2* (SKY646) cells were starved for 30 min. After addition of 0 or 0.2 µg/ml rapamycin, the cells were cultured for an additional 24 h, lysed, and subjected to western blot analysis. A representative blot of two independent experiments is shown. Arrowhead indicates a non-specific band. (B) WT (BY4741) and Δ*atg1* (YKOL7090) cells expressing pRS316/Atg1 WT or kinase-dead mutant (KD; D211A) were starved for 30 min or 24 h, and then lysed and subjected to western blot analysis. A representative blot of two independent experiments is shown. (C) FLAG-tagged Atg1 WT or kinase-dead mutant (D211A) purified from rapamycin-treated cells was incubated with TAP-tagged Atg13 purified from Δ*atg1* cells in the presence of radiolabeled ATP. A representative image of two repeats is shown. (D) Atg13–TAP proteins were purified from WT (SKY721) and Δ*atg1* (SKY722) grown for 24 h in nutrient-rich medium or under starvation conditions. Atg13–TAP proteins were digested in-gel, and phospho-peptides were concentrated and subjected to mass spectrometry. The abundances of detected Atg13 phospho-peptides are shown. Values were normalized against wild type, defined as 1. N.D., not detected. (E) Δ*atg13* (YKOL5600), Δ*atg9* (YKOL3847) and Δ*atg1* (YKOL4547) cells in nutrient-rich conditions and WT (BY4741) cells starved for 0, 0.5, 2, 6, 12, or 24 h were subjected to western blotting using the indicated antibodies. For Phos-tag PAGE, 15 µM Phos-tag was included in the SDS-PAGE gel. A representative blot of three independent experiments is shown. (F) WT (TNY509), Δ*ptc1-4* (SKY773), Δ*ptc1-4*Δ*atg1* (SKY785) and Δ*ptc1-4*Δ*atg13* (SKY783) cells starved for 0 or 2 h were subjected to western blotting with the indicated antibodies. Left and right panels show independent blots, each representative of two independent experiments.

in Atg13 re-phosphorylation, although Δ*atg16* exhibited a mild defect (Fig. S2A). These data strongly suggest that the defect in Atg13 re-phosphorylation in Δ*atg1* under persistent starvation is not due to a defect in autophagy, but instead dependent on the lack of Atg1 itself. The kinase activity of Atg1 is important for Atg13 re-phosphorylation because expression of the *ATG1* kinase-dead mutant did not complement the Atg13 re-phosphorylation defect (Fig. 2B). An *in vitro* kinase assay revealed that Atg13 was phosphorylated by the purified Atg1 protein, but not by the kinase-dead mutant protein (Fig. 2C). We also confirmed that Atg13 S379 and S428/S429, which are critical moieties for pre-autophagosomal structure, also known as phagophore assembly site (PAS), formation and induction of autophagy (Fujioka et al., 2014; Yamamoto et al., 2016), were phosphorylated by purified Atg1 *in vitro* (Fig. S2B). Furthermore, mass spectrometry analysis revealed that the abundance of Atg13 phospho-peptides was significantly lower in Δ*atg1* cells than in wild-type cells after starvation for 24 h (Fig. 2D), while there was only a modest effect in nutrient-rich conditions (Fig. S2C). Taken together, these data indicate that Atg1 kinase re-phosphorylates Atg13 under persistent starvation.

Next, we compared the phosphorylation time course of Atg1 substrates. Atg9 is phosphorylated by Atg1 kinase, and its phosphorylation is important for autophagic activity (Papinski et al., 2014). We utilized Phos-tag PAGE to monitor Atg9 phosphorylation, as previously reported (Yamamoto et al., 2016). After starvation for 2 h, Atg9 was already phosphorylated, but Atg13 re-phosphorylation was barely detectable (Fig. 2E). This data indicates that the timing of phosphorylation by Atg1 kinase differs among the substrates. To further analyze the difference in phosphorylation patterns among Atg1 substrates during starvation, we investigated PP2C phosphatases, which can dephosphorylate Atg13 (Fujioka et al., 2020; Memisoglu et al., 2019). Among seven PP2C genes, we constructed a quadruple deletion mutant (Δ*ptc1-4*) of *PTC1*, *PTC2*, *PTC3* and *PTC4*, which encode proteins located in the cytosol rather than the mitochondria. In Δ*ptc1-4* cells, Atg13-S379 was phosphorylated even after 2 h of starvation (Fig. 2F). In western blots with anti-Atg13 antibody, an upshifted band of ∼150 kDa appeared, but disappeared upon deletion of *ATG13*, suggesting that it represents a hyper-phosphorylated form of Atg13 (Fig. 2F, right panel). Additional deletion of *ATG1* in Δ*ptc1-4* eliminated phosphorylation of Atg13-S379 and the hyper-phosphorylated form of Atg13, indicating that Atg13 phosphorylation at the earlier time point of starvation was mediated by the Atg1 kinase. Consistent with the positive role of PP2C in these processes, under starvation, Ptc2 formed puncta (Fig. S2D) that were colocalized with PAS marker proteins Atg13 and Ape1 (Fig. S2E). By contrast, the phosphorylation status of Atg9, another Atg1 substrate, was barely affected in Δ*ptc1-4* under starvation (Fig. S2F). Collectively, these findings indicate that PPC2 phosphatases specifically affect phosphorylation of Atg13, which regulates autophagy termination.

Identification of *TAG1* as a gene responsible for autophagy termination

To search for other factors responsible for autophagy termination, we surveyed autophagic activity in two kinds of genome-wide yeast mutant collections – one in which each non-essential gene has been individually deleted, and another in which mRNA expression of each essential gene is decreased due to a disruption in the 3′UTR (Schuldiner et al., 2005). A total of 5761 mutant strains were cultured on YEPD agar plate medium, and then shifted for nitrogen starvation, and ALP activity was measured at 0, 4 and 24 h (Fig. 3A,B; Table S1). As we had reported in previous studies, almost all of the core Δ*atg* mutants, which are fully defective in starvation-induced autophagy, were among the strains with the lowest autophagic activities after 4 h of starvation (Kira et al., 2014; Shirahama-Noda et al., 2013). Ksp1 is a protein kinase that negatively regulates autophagy through activation of TORC1, and Δ*ksp1* cells also had high autophagic activity after 24 h of starvation (Table S1) (Umekawa and Klionsky, 2012). Notably, several vacuolar ATPase–deficient mutants (Δ*vma2*, Δ*vma5*, Δ*vma7*, Δ*vma8*, Δ*vma10*, Δ*vma22*, etc.) had higher autophagic activity at 0, 4 and 24 h (Table S1). We performed secondary screening using an ALP assay with more carefully cultured cells in YEPD liquid medium against top 50 highest ALP activities and starved for 24 h. Based on the results of the secondary screen, we decided to focus on one uncharacterized gene, *YLR173W*, whose mutant had 1.9-fold higher ALP activity than wild type after starvation for 24 h; it had the 8th highest activity overall in the primary screen, and the 7th highest in the secondary screen. We named *YLR173W TAG1* (for Termination of AUTOPHAGY) based on the following results. In a time course analysis of Δ*tag1* cells, ALP activity increased until 8 h of starvation, just like in wild-type cells, but exhibited no decrease after 8 h (Fig. 3C). Thus, the higher ALP activity in Δ*tag1* cells reflects a defect in termination of autophagy, rather than higher basal activity or accelerated autophagy during earlier time points. To confirm these findings, we examined autophagic bodies, which are inner membrane structures of autophagosomes after delivery into the vacuole; these bodies disintegrate immediately after release into the vacuolar lumen, but are kept intact by treatment with the protease inhibitor PMSF (Takeshige et al., 1992). Using a conditional gene expression system for GFP–Atg8 (McIsaac et al., 2013), we observed autophagic bodies that accumulated after persistent starvation. After starvation for 12 h, estradiol was added to induce GFP–Atg8 expression, and PMSF was simultaneously added to block degradation of autophagic bodies in the vacuole. GFP–Atg8 was indeed induced after starvation for 15 h (Fig. S3A). In wild-type cells, quite a few autophagic bodies accumulated, indicating that autophagy had been terminated (Fig. S3B, Movie 1). However, a number of autophagic bodies clearly accumulated in Δ*tag1* cells (Fig. S3B, Movie 2). Therefore, we concluded that *TAG1* is responsible for autophagy termination.

Journal of Cell Science (2021) 134, jcs253682. doi:10.1242/jcs.253682

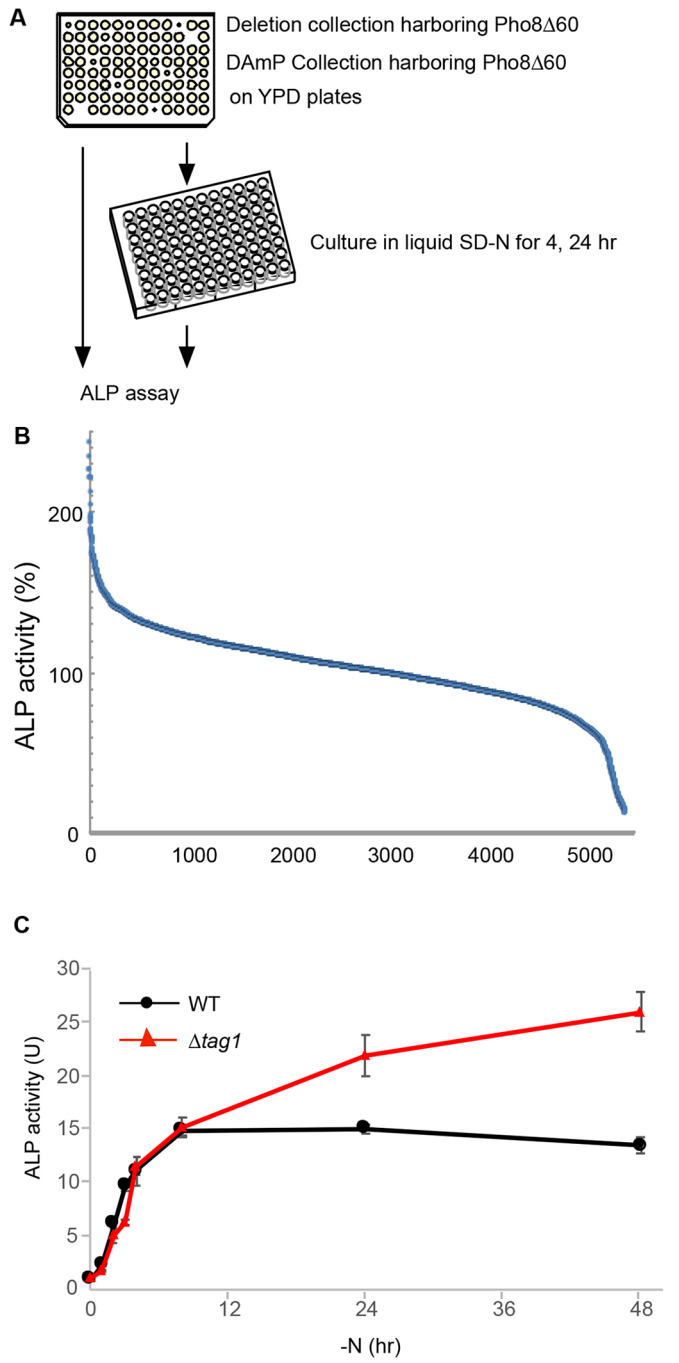

Fig. 3. Identification of Tag1, which is responsible for autophagy termination. (A,B) Genome-wide screening for genes responsible for autophagy regulation. (A) Schematic diagram of the screen. Cells from the yeast knockout library or the DAmP knockdown library harboring the Pho8Δ60 allele instead of wild-type PHO8 were cultured on YPD plates, and then either subjected to an ALP assay directly or starved for 4 or 24 h before the ALP assay. (B) Screen results. ALP activity after 24 h of starvation. Data represent relative ALP activities; wild type was defined as 100%. (C) Wild-type (WT; TNY509) and Δ*tag1* (MNY001) cells were incubated in SD-N (pH 6.2) and subjected to an ALP assay at the indicated time points over 48 h. Results are shown as mean±s.d. (*n*=3).

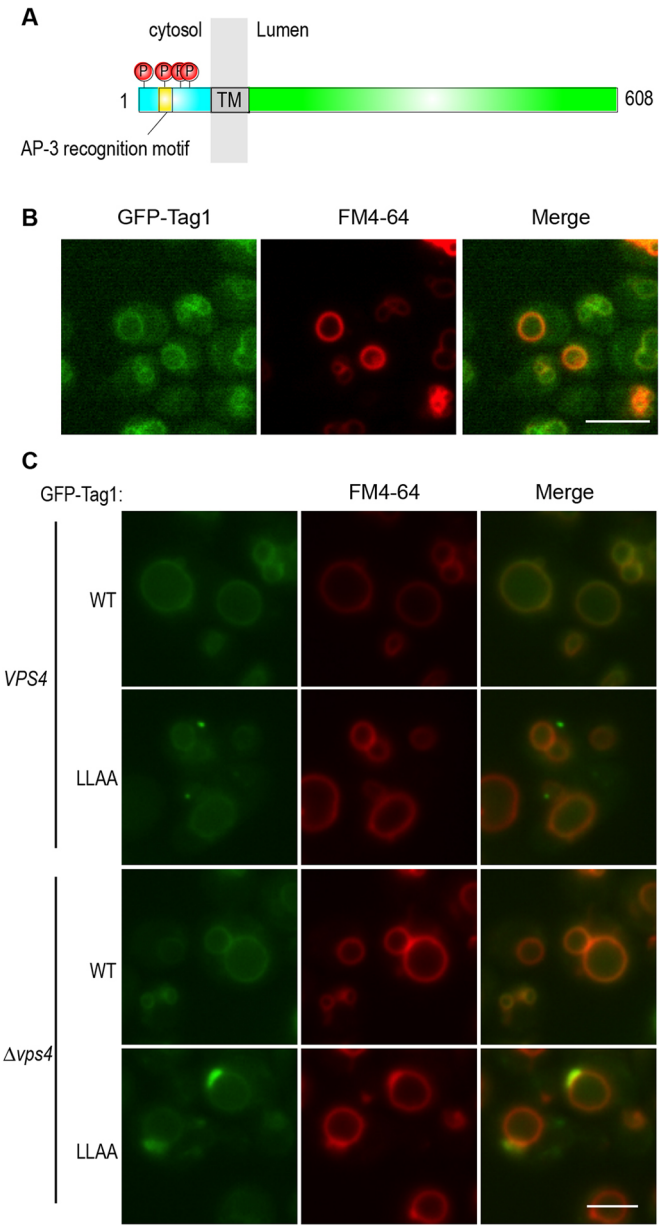

Fig. 4. Tag1 is a vacuolar membrane protein that forms perivacuolar foci dependent on autophagy under prolonged starvation. (A) Schematic diagram of Tag1 primary sequence. The Tag1 cytosolic domain contains an AP-3 recognition motif and predicted phosphorylation sites. (B) GFP–Tag1-expressing cells (MNY069) stained with FM4-64 were subjected to microscopy. (C) Δ*tag1* (MNY029) and Δ*tag1*Δ*vps4* (SKY700) cells harboring GFP–Tag1 WT and the AP-3 recognition motif mutant (pSK402 and pSK540) stained with FM4-64 and imaged by microscopy. Scale bars: 5 µm.

Tag1 is a vacuolar membrane protein

TAG1 encodes a 608-amino-acid protein with a single hydrophobic stretch appropriate for a transmembrane region [amino acids (aa) 54–75] (Fig. 4A). In a previous proteomics analysis of isolated yeast vacuoles, Tag1 was identified as a potential vacuolar-localized protein (Wiederhold et al., 2009). Consistent with this, N-terminally GFP-tagged Tag1 under the control of its own promoter was localized along the vacuolar membrane (Fig. 4B). Two facts confirm that Tag1 is a vacuolar type II membrane protein with the N-terminal region oriented toward the cytosol and the C-terminus inside the lumen. First, previous phospho-proteomic analysis revealed phosphorylation sites only in the N-terminal region (S5, T16, T24, S27) (Fig. 4A) (Albuquerque et al., 2008; Holt et al., 2009; Swaney et al., 2013). Second, there is a possible adaptor protein complex 3 (AP-3) recognition motif ([D/E]XXXL[L/V]) that could act as a vacuolar

Journal of Cell Science (2021) 134, jcs253682. doi:10.1242/jcs.253682

targeting signal in the N-terminal region (aa 15–20, ETQPLL) (Cowles et al., 1997). We replaced the di-leucine with di-alanine (aa 15–20, ETQPAA), resulting in a slight defect in vacuolar localization (Fig. 4C) (Darsow et al., 1998). In combination with deletion of Δ*vps4*, the di-leucine mutant of GFP–Tag1 was not delivered to the vacuole, but instead accumulated in a perivacuolar structure stained with FM4-64, a feature of the class E compartment (Fig. 4C), whereas wild-type GFP–Tag1 was delivered normally even in Δ*vps4*, implying that the di-leucine mutant bypassed the vacuole via the CPY pathway. These observations indicate that the ETQPLL motif is a functional AP-3 recognition motif on the cytoplasmic side.

Cleavage of its luminal region leads to dysfunction of Tag1

N-terminally 3HA-tagged Tag1 expressed from its native promoter could be detected as a 116-kDa band on immunoblots (Fig. 5A). Endoglycosidase H treatment resulted in a mobility shift to 81 kDa, indicating that Tag1 is modified by N-linked sugar chains in the luminal domain (Fig. S4A). In addition to the 116 kDa band, we also detected bands at 21 kDa and 50 kDa (Fig. 5A). These bands were not observed in cells lacking Pep4, the vacuolar proteinase A, which processes various vacuolar enzymes to activate them (Fig. 5A) (Hecht et al., 2014). Therefore, these bands must be generated by cleavage, either directly by Pep4 or by other vacuolar proteases activated by Pep4. Based on the molecular masses, the cleavage is predicted to occur at the luminal domain, close to the transmembrane domain.

To narrow down the cleavage sites, several C-terminal deletion constructs at or around the predicted sites were generated, tagged with FLAG at N-terminus and with HA at C-terminus, and expressed in cells with or without the major vacuolar proteases Pep4 and Prb1 (Hecht et al., 2014) (Fig. S4B). Even the shortest C-terminal deletion mutant, truncated to 80 aa, yielded the cleaved form in the presence of Pep4 and Prb1, but not in absence of Pep4 and Prb1 (Fig. S4B). A construct that lacks the 23 amino acid residues following the transmembrane region (Δ77–90) was also cleaved (Fig. S4C). These observations suggest that the cleavage occurs at the luminal region adjacent to the transmembrane domain in a sequence-independent manner.

To determine the significance of Tag1 processing, we replaced the endogenous Tag1 with a variety of Tag1 luminal-domain deletion mutants (Fig. 5B). Although the full-length Tag1 construct fully complemented the autophagy termination defect in Δ*tag1* cells (Fig. S4D), all of the other luminal deletion mutants failed to complement Tag1 function (Fig. 5B,C), despite vacuolar localization of these mutants being maintained (Fig. 5D; Fig. S5G). These data imply that most luminal regions are required for its function. Nevertheless, the cleaved 21-kDa form was generated in cells expressing all of these deletion constructs (Fig. S4E), indicating that the cleaved 21-kDa form alone could not support Tag1 function.

To determine the importance of the other portion of Tag1, we replaced each domain of Tag1 with Pho8, an alkaline phosphatase and vacuolar membrane protein with the same orientation as Tag1 (Huang et al., 2015; Klionsky and Emr, 1989) (Fig. 5E). These constructs, tagged with GFP, were expressed in place of the native *TAG1* gene. All constructs localized along the vacuolar membrane under nutrient-rich conditions (Fig. 5G). Wild-type GFP-Tag1 fully complemented Tag1 function, but replacement of the luminal domain with Pho8 in which the catalytic center was mutated, in order to avoid interference with the ALP assay (Kira et al., 2016), prevented complementation, as expected from the results described above (Fig. 5F). On the other hand, the variant in which the transmembrane domain was replaced with Pho8 could complement Tag1 function (Fig. 5F). Strikingly, complementation also occurred when the cytosolic domain was replaced with Pho8 (Fig. 5F). These data indicate that both the cytosolic and transmembrane domain are dispensable for Tag1 function, or at least interchangeable with an unrelated vacuolar membrane protein.

These results raised two possibilities, (1) that the luminal domain could function even as a cleaved soluble form in the vacuolar lumen, or (2) that the luminal domain must be connected to the transmembrane and cytosolic domains, but these are replaceable with an unrelated protein. To discriminate between these two possibilities, we artificially targeted the Tag1 luminal domain into vacuolar lumen. The vacuolar enzyme carboxypeptidase S is transported into the vacuolar lumen via the multivesicular body pathway, and its C-terminal pro-region is cleaved off by Pep4 (Katzmann et al., 2001; Odorizzi et al., 1998). We made a fusion protein of CPS and the GFP–Tag1 luminal domain (Fig. 5H). The fusion protein was transported into the vacuolar lumen (Fig. 5J), but did not complement the Δ*tag1* autophagic termination defect (Fig. 5I). Therefore, the Tag1 luminal domain connected to the transmembrane domain in the vacuolar membrane is required for full Tag1 function.

Tag1 forms foci in the vacuole membrane during starvation

We next noticed that, under starvation, vacuolar membrane GFP–Tag1 signals became less intense, and mostly gathered in a single punctum in the vacuolar membrane, in a time-dependent manner (Fig. S5A–D). Foci formation was not observed for GFP–Pho8, implying that it is not general phenomena (Fig. S5E). These foci were not more abundant in the autophagy-defective mutant Δ*atg7* (Fig. S5A,B), indicating that autophagy plays a positive role in formation of Tag1 foci. By contrast, the foci do not overlap with the Atg13–mCherry signal, a marker of the PAS, where autophagosome formation takes place (Fig. S5F), and no physical interaction was detected between Tag1 and Atg1 (Fig. S5G). We observed no significant colocalization of GFP–Tag1 foci and various perivacuolar organelle markers (Fig. S5H).

Next, we sought to determine which domain of Tag1 is important for foci formation. To this end, we used truncation mutants and domain-swap mutants with Pho8 (Fig. 5D,G; Fig. S5G,I). Luminal domain truncation mutants did not form foci (Fig. 5D; Fig. S5I). The cytosolic and transmembrane domain-swapped mutants formed foci, whereas the luminal domain-swapped mutant failed to do so (Fig. 5G; Fig. S5J). These data support the idea that the luminal domain is important for foci formation.

Tag1 protein level is maintained through microautophagic degradation and synthesis, which affects autophagy termination

We next found that autophagy termination was also defective when Tag1 was overexpressed from the strong GPD promoter (Fig. 6A), suggesting that the amount of Tag1 must be maintained within some proper range in order for the protein to fulfill its function. On the other hand, the level of *TAG1* mRNA was elevated under nitrogen starvation (Fig. 6B). Nevertheless, the level of Tag1 protein, both the uncleaved 116-kDa form and the cleaved 21-kDa fragment, was not increased during starvation (Fig. 5A). When protein synthesis was inhibited by cycloheximide treatment, the Tag1 protein level decreased during starvation (Fig. 6C). These observations prompted us to hypothesize that the Tag1 protein level is maintained by balancing protein synthesis and degradation during starvation.

When GFP–Tag1 was expressed in Δ*pep4* cells, the GFP signal was detected in the vacuolar lumen during starvation (Fig. 6D). In

Journal of Cell Science (2021) 134, jcs253682. doi:10.1242/jcs.253682

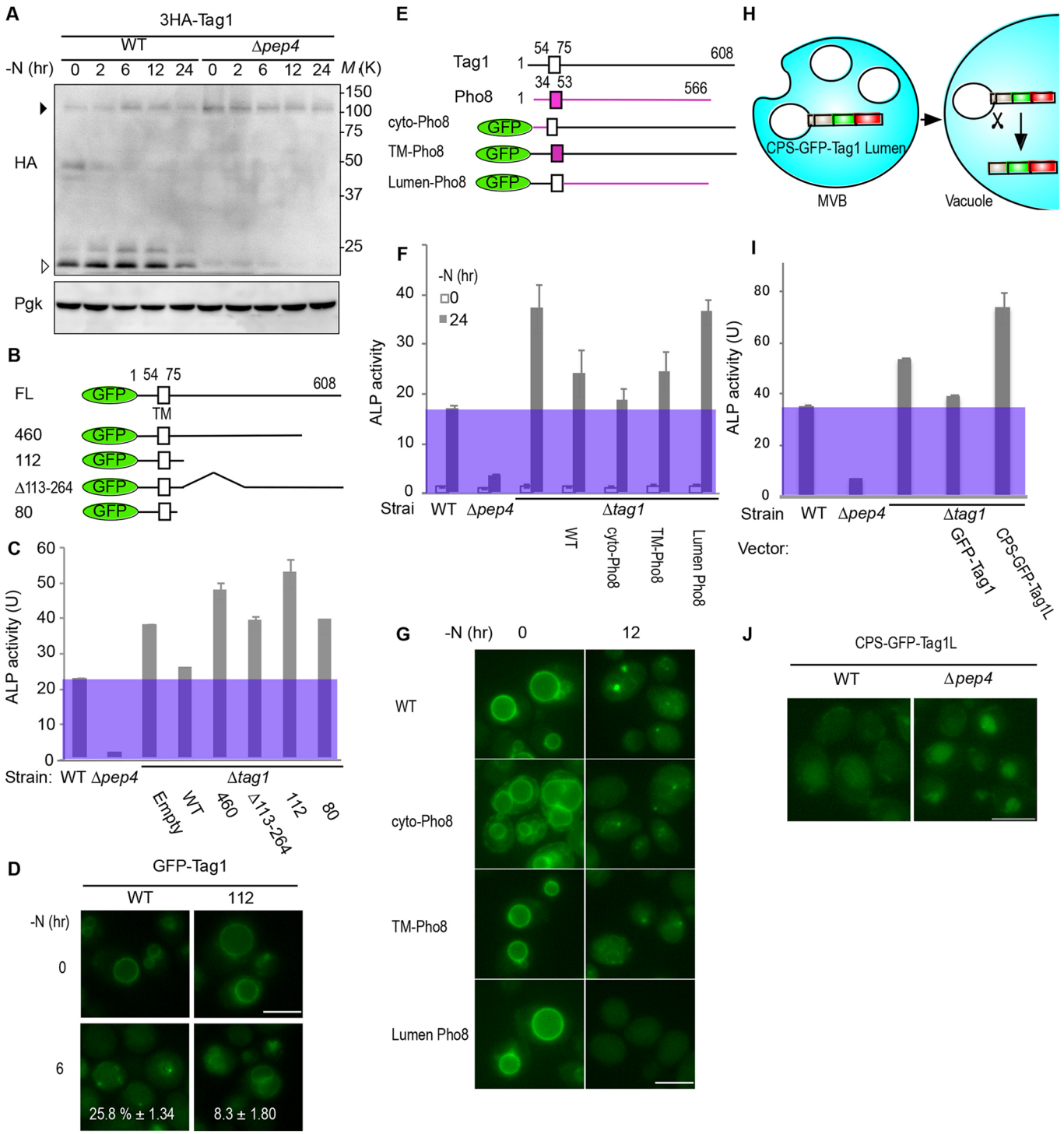

Fig. 5. The Tag1 luminal domain is important for autophagy termination. (A) Wild-type (WT; BY4741) and Δ*pep4* (YKOL2098) cells harboring pRS316/3HA-Tag1(pSK442) were starved in SD-N (pH 6.2) for 2, 6, 12, or 24 h and subjected to western blot analysis. A representative blot of three independent experiments is shown. (B) Schematic diagram of GFP–Tag1 truncated mutants. (C) WT (TNY509), Δ *pep4* (SKY001) and Δ*tag1* (MNY001) cells harboring GFP–Tag1 wild type (pSK402) or truncation mutants [1460 aa (pSK447), 1–112 aa (pSK449), Δ113–264 aa (pSK450), 1–80 aa (pSK499)] were starved in SD-N (pH 6.2) for 24 h and subjected to an ALP assay (mean±s.d.; *n*=3). (D) Δ*tag1* (MNY029) cells harboring pRS316/GFP-Tag1(pSK402) and pRS316/GFP-Tag1 1–112 aa (pSK449) were starved for 6 h and subjected to microscopy. Perivacuolar dots were counted. For each sample, 150–250 cells were counted, and data represent means±s.d. from three independent experiments. (E) Schematic diagram of domain-swap mutants of Tag1 with Pho8. (F) WT (TNY509), Δ*pep4* (SKY001), and Δ*tag1* (MNY029) cells harboring pRS316/GFP-Tag1 (pSK402) and domain-swap mutants with Pho8 [pRS316/GFP-Tag1 cyto-Pho8(pSK404), pRS316/GFP-Tag1 TMD-Pho8(pSK405), pRS316/GFP-Tag1 lumen-Pho8 (Δ120–128) (pSK408)] were starved in SD-N (pH 6.2) for 24 h and subjected to an ALP assay (mean±s.d.; *n*=3). (G) BY4741 cells harboring pSK402, 404, 405 or 408 were starved in SD-N (pH 6.2) for 12 h and subjected to microscopy. (H) Schematic of the fusion protein CPS–GFP–Tag1 and its localization. (I) WT (TNY509), Δ*pep4* (SKY001) and Δ*tag1* cells harboring pSK402 and pRS426/pTag-CPS-GFP-Tag1 Lumen (pSK508) were starved for 24 h, and subjected to an ALP assay (mean±s.d.; *n*=3). (J) BY4741 and Δ*pep4* cells harboring pSK508 were cultured in SCD and subjected to microscopy. Scale bars: 5 µm.

Journal of Cell Science (2021) 134, jcs253682. doi:10.1242/jcs.253682

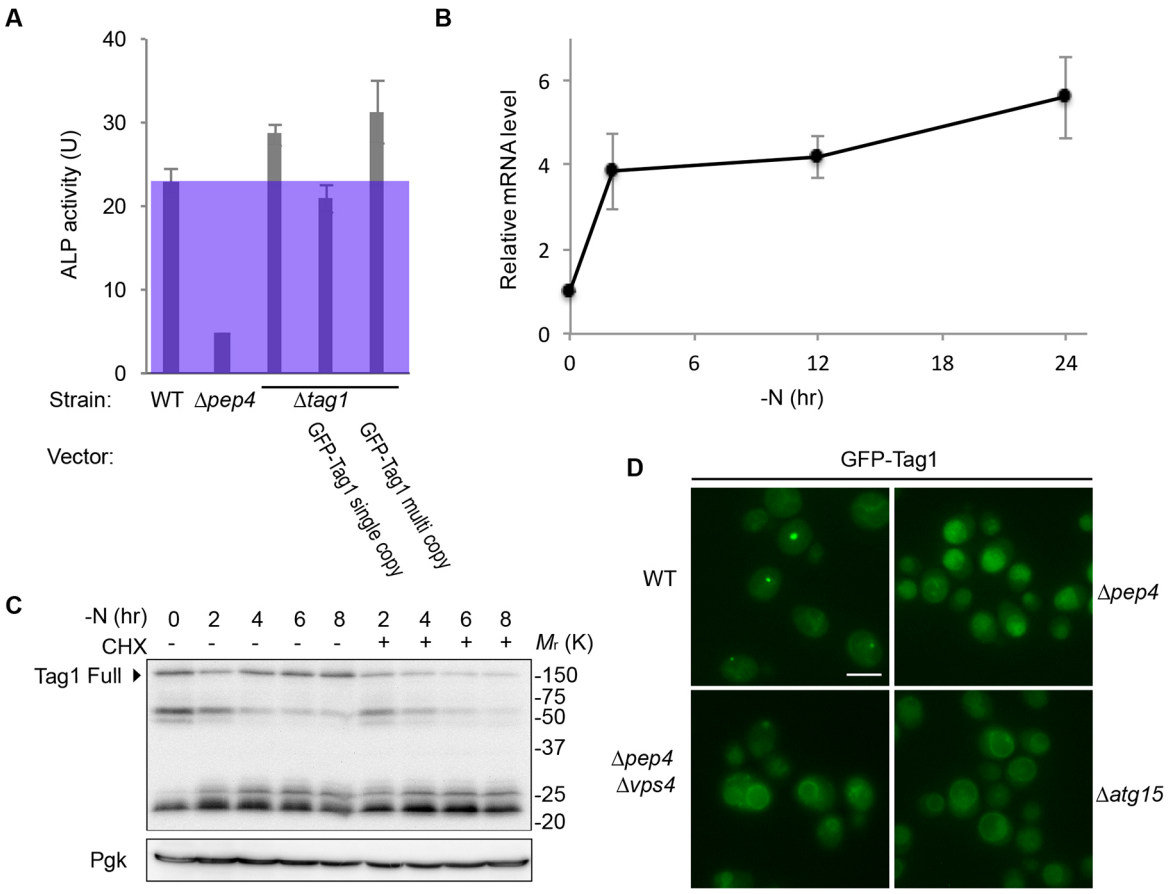

Fig. 6. Tag1 protein level is important for autophagy termination. (A) Wild-type (WT; TNY509), Δ*pep4* (SKY001) and Δ*tag1* (MNY001) cells harboring empty vector, pRS316/GFP–Tag1 (pSK402), and pRS426/GFP-Tag1 (pSK507) were cultured in SD-N (pH 6.2) for 24 h and subjected to an ALP assay (mean±s.d.; *n*=3). (B) BY4741 cells were starved for 2, 12, or 24 h; the cells were lysed, and total RNA was harvested and subjected to qPCR analysis. mRNA levels are shown relative to those in nutrient-rich conditions (mean±s.d.; *n*=3). (C) MNY029 (BY4741, Δ*tag1*) cells expressing pRS316/3HA-Tag1 (pSK442) were starved for 2, 4, 6 or 8 h with or without 50 µM cycloheximide and subjected to western blot analysis. A representative blot of three independent experiments is shown. (D) GFP–Tag1 cells [WT (MNY069), Δ *pep4* (SKY555), Δ*pep4* Δ*vps4* (SKY565) and Δ*atg15* (SKY573)] were starved for 12 h and subjected to microscopy. Scale bar: 5 µm.

mutants of the vacuolar lipase Atg15, which is responsible for disintegration of vacuolar luminal vesicles such as autophagosomes and multivesicular bodies (Epple et al., 2001), GFP–Tag1 also accumulated in the lumen (Fig. 6D). However, GFP–Pho8 also exhibited such accumulation in Δ*pep4* cells (Fig. S5C). The Tag1 lumen-swapped mutant, which was defective in Tag1 foci formation, also showed accumulation of GFP signals in the vacuole in Δ*pep4* cells (Fig. S5H), indicating that Tag1 foci formation is dispensable for vacuolar accumulation. This vacuolar luminal signal could not be detected in the double mutant of *VPS4*, which encodes a protein engaged in the endosomal sorting complexes required for transport (ESCRT)-dependent process, and *PEP4* (Fig. 6D) (Oku et al., 2017; Zhu et al., 2017). Thus, a fraction of GFP–Tag1, and possibly also other vacuolar membrane proteins, such as Pho8, was incorporated into the vacuolar lumen via ESCRT-dependent microautophagy under nitrogen starvation, as observed for the vacuolar membrane proteins Vph1 and Pho8 during the diauxic shift (Oku et al., 2017; Zhu et al., 2017). This mechanism would be expected to maintain the proper amount of Tag1 in the vacuolar membrane under nitrogen starvation.

Tag1 regulates PAS disassembly by Atg13 re-phosphorylation under persistent starvation

Next, we examined the effect of *TAG1* gene deletion on Atg proteins. We first monitored the levels of Atg proteins in wild-type yeast cells, and found that most Atg proteins became more abundant during persistent starvation (Fig. S6A). Therefore, the decrease in the Atg protein level does not seem to be the cause of autophagy termination in yeast. Of note, Atg1 expression level increased under starvation (Fig. S6B), despite a previous report showing that the Atg1 level was reduced due to autophagic degradation (Kraft et al., 2012). The increase in Atg1 protein levels during starvation was suppressed by cycloheximide treatment (Fig. S6B), indicating that Atg1 expression is upregulated under starvation. In combination with evidence that Atg1 is degraded by autophagy (Kraft et al., 2012; Nakatogawa et al., 2012b), this implies that the Atg1 protein synthesis level is higher than the rate of degradation by autophagy during starvation.

We also investigated whether Tag1 affects Atg1 kinase activity by using Phos-tag PAGE to monitor Atg1 autophosphorylation and phosphorylation of its substrates Atg9 and Atg29. We confirmed that phosphorylation of Atg9 and Atg29 were dependent on Atg1 (Mao et al., 2013; Papinski et al., 2014) (Fig. S6D; Fig. S6E, right panel). However, we detected no significant difference between wild-type and Δ*tag1* cells (Fig. S6C–E).

We then investigated whether *TAG1* affects Atg13 re-phosphorylation, focusing on phosphorylation sites critical for regulation of autophagy (Fujioka et al., 2014; Yamamoto et al., 2016). Atg13 S379 and S428/S429 dephosphorylation is critical for the interaction between Atg13 and Atg17, as well as for autophagy

Journal of Cell Science (2021) 134, jcs253682. doi:10.1242/jcs.253682

(Fujioka et al., 2014; Yamamoto et al., 2016). This phosphorylation disappeared upon rapamycin treatment, suggesting that TORC1 is responsible for S379 phosphorylation, at least under nutrient-rich conditions (Yamamoto et al., 2016). Under such conditions, Atg13-S379 was also phosphorylated in Δ*tag1* cells, but this band disappeared after 30 min of starvation (Fig. 7A). In wild-type cells, Atg13-Se379 re-phosphorylation was observed after 24 h of starvation (Fig. 7A). However, re-phosphorylation of Atg13-S379 was significantly lower in Δ*tag1* than in the wild type (Fig. 7A), although overall Atg13 re-phosphorylation was not significantly altered in Δ*tag1* cells (Fig. 7A, upper panel). We also monitored the phosphorylation status of Atg13 S428/S429, another critical phosphorylation site for autophagy regulation (Fujioka et al., 2014). Re-phosphorylation of Atg13 S428/S429 was also significantly reduced in Δ*tag1* cells (Fig. S6F). Taken together, these observations indicate that Tag1 affects re-phosphorylation of the crucial sites S379 and S428/S429 under persistent starvation.

We next asked whether Atg13-S379 phosphorylation status is sufficient for control of autophagic termination. Cells expressing the dephosphorylation mimic mutant Atg13-S379A terminated autophagy normally, and no additive effect was observed in Δ*tag1* cells expressing Atg13-S379A (Fig. S6G). Furthermore, the general re-phosphorylation pattern of Atg13 was barely affected in cells expressing Atg13-S379A (Fig. S6H). These data indicate that dephosphorylation of the Atg13-

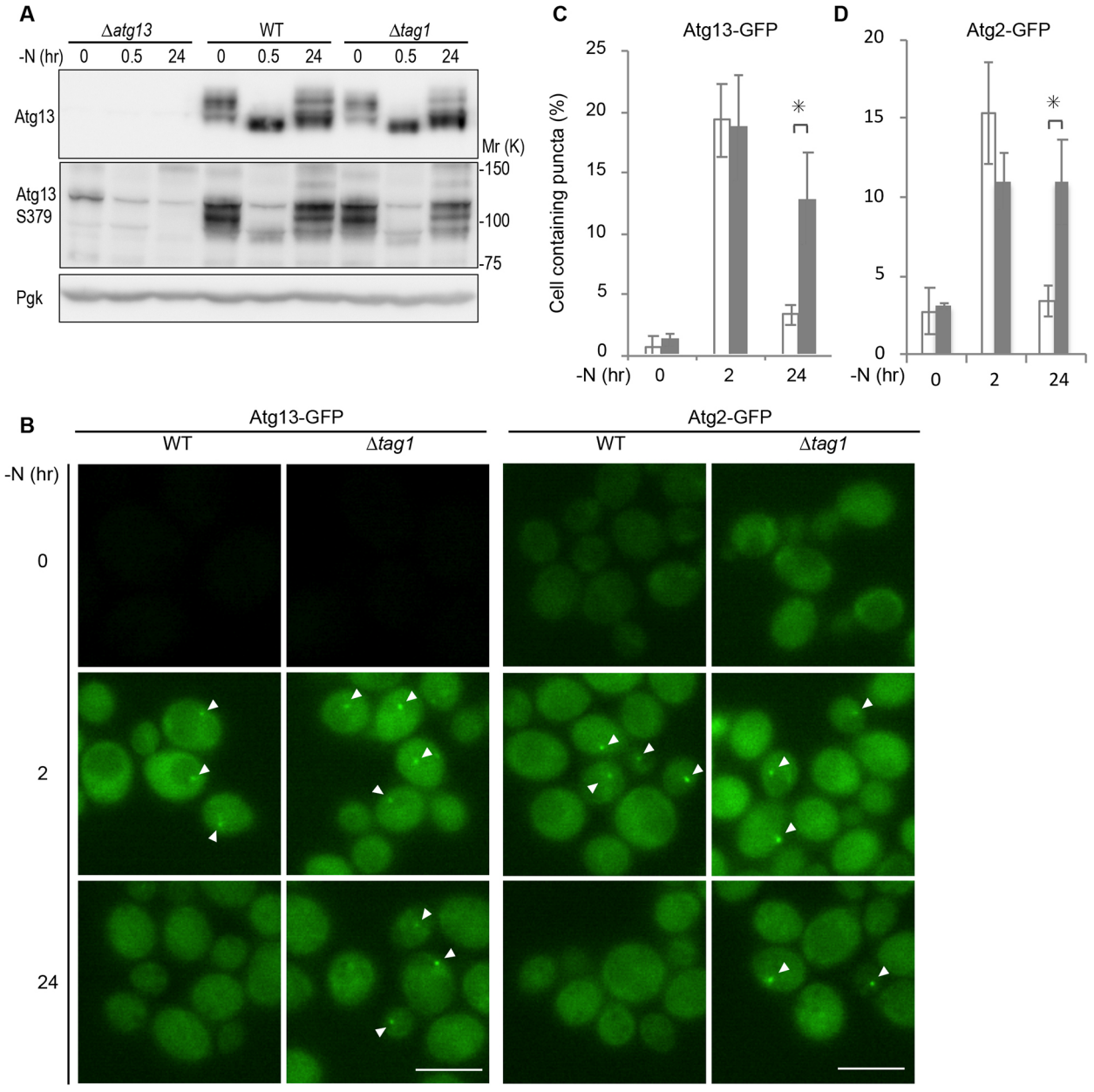

Fig. 7. Tag1 is required for Atg13 re-phosphorylation and PAS disassembly under persistent starvation. (A) Δ*atg13* (YKOL4547), wild-type (WT; BY4741) and Δ*tag1* (MNY029) cells were starved for 30 min or 24 h, lysed, and subjected to western blot analysis. A representative blot of four independent experiments is shown. (B) Atg13–GFP and Atg2–GFP puncta (arrowheads) in WT and Δ*tag1* cells deleted for *ATG11* [Atg13, WT (SKY139) and Δ*tag1* (MNY062); Atg2, WT (MNY100) and Δ*tag1* (MNY102)] were cultivated in SCD or starved for 2 or 24 h, and then subjected to microscopy. Scale bars: 5 µm. (C,D) Atg13–GFP and Atg2–GFP puncta in (B) were counted, and the results were expressed as percentages. For each sample, 200–300 cells were counted, and data represent means±s.d. from three independent experiments. **P*<0.02 (two-tailed paired Student's *t*-test).

S379 moiety itself is not sufficient for autophagic termination. We also tested the Atg13-S379A, S428A, S429A triple mutant; however, no significant effect was observed (Fig. S6H).

Next, we investigated the localization of Atg proteins in Δ*tag1* cells. *ATG11* was deleted to discriminate Atg assembly at PAS dependent on starvation-induced autophagy from that involved in the CVT pathway (Kawamata et al., 2008; Shintani and Klionsky, 2004). In wild-type cells, perivacuolar puncta of Atg13–GFP and Atg2–GFP (representing the PAS) were induced after 2 h of starvation (Fig. 7B–D). However, the proportion of cells showing Atg13–GFP and Atg2–GFP puncta was significantly decreased after 24 h starvation (Fig. 7B–D). Thus, Atg proteins eventually disassemble from the PAS under persistent starvation, leading to termination of autophagy. In Δ*tag1* cells, Atg13 puncta were formed in 2 h, as in wild-type cells; however, a significant number of cells contained Atg13–GFP puncta even after 24 h of starvation (Fig. 7B,C). Similar results were obtained with Atg2 (Fig. 7B,D). Thus, Tag1 affects Atg disassembly from the PAS under persistent starvation. Collectively, these data imply that Tag1 affects phosphorylation of Atg13, leading to PAS disassembly and autophagy termination under persistent starvation.

DISCUSSION

In this study, we sought to determine how autophagy is terminated under nitrogen starvation in yeast. Yeast appear not to employ either of the two mechanisms for autophagy termination proposed for mammalian cells, that is, mTORC1 reactivation or degradation of ATG proteins by the proteasome (Antonioli et al., 2014; Liu et al., 2016; Nazio et al., 2016; Yu et al., 2010). Inactivation of TORC1 at the reactivation phase did not affect autophagy termination (Fig. 1C), and rather than being degraded, ATG proteins were upregulated during the termination period (Fig. S6A–C). Thus, yeast seem to use an unexplored mechanism for autophagy termination involving Tag1. No obvious homolog of Tag1 exists outside of fungi, suggesting that the termination mechanism differs between yeast and mammals.

Re-phosphorylation of Atg13 under persistent starvation was defective in cells lacking Atg1 kinase activity (Shin and Huh, 2011), and was not mediated by TORC1 but rather by Atg1 kinase (Figs 2A,B and 1D; Fig. S1C). This is reasonable, as Atg1 and Atg13 form a complex during starvation. Because PAS formation is suppressed by phosphorylation of critical moieties of Atg13 (Fujioka et al., 2014; Kamada et al., 2009; Yamamoto et al., 2016), autophagy termination could be mediated by re-phosphorylation of this protein. Indeed, re-phosphorylation of these critical moieties was defective in Δ*atg1* cells (Fig. 2A,D; Fig. S6F). Furthermore, these moieties of Atg13 were phosphorylated by Atg1 *in vitro* (Fig. S2B). Consistent with this, the PAS scaffold protein complex Atg13–Atg17–Atg29–Atg31 assembles as a liquid droplet, and phosphorylation of Atg13 by Atg1 disassembles this liquid droplet *in vitro* (Fujioka et al., 2020). We observed that the PAS disappeared under persistent starvation (Fig. 7B–D). We also showed that PP2C phosphatases play a negative role in this regulation of Atg13, but not in regulating the other Atg1 substrate, Atg9 (Fig. 2E; Fig. S2D,E). Therefore, dispersion of PAS mediated re-phosphorylation of Atg13 by Atg1 serves as a 'safety timer'-like mechanism that prevents overshoot of autophagy.

Another crucial factor is the novel vacuolar protein Tag1. In the Δ*tag1* mutant, Atg13 re-phosphorylation is defective, leading to suppression of PAS dispersion and autophagy termination (Fig. 7). Thus, there must exist a mechanism that links Tag1 to the Atg1–Atg13 axis. How does Tag1 regulate Atg13 re-phosphorylation? We could not detect any difference in Atg1 kinase activity in Δ*tag1* cells, nor could we demonstrate any physical interaction between Atg1 and Tag1 (Figs S6C–E, S5E). Another possibility is that Tag1 affects PPC2 phosphatase activity toward Atg13. Atg13 is gradually re-phosphorylated during starvation, even in the presence of PP2C phosphatase (Fig. S1C), possibly because phosphatase activity is decreased. Given that Atg13 re-phosphorylation is affected in the Δ*tag1* mutant, one hypothesis is that Tag1 suppresses PPC2 phosphatase during starvation; this should be clarified in future work.

The Tag1 luminal domain was crucial, and needed to be connected to the membrane and cytosolic domains (Fig. 5). Therefore, the most plausible mechanism is that Tag1 luminal domain is affected by the outcome of autophagy inside the vacuolar lumen; for example, amino acids produced by protein degradation. This hypothesis is supported by the observation that Tag1 foci formation was defective in the Δ*atg7* mutant (Fig. S5A–C), indicating that Tag1 responds to the progression of autophagy at least in terms of its localization. This is further supported by the observation that the luminal domain is necessary for foci formation (Fig. 5D,G; Fig. S5G,H). The Tag1 protein amount is determined by the balance between the *de novo* synthesis of the Tag1 protein and microautophagic degradation (Fig. 6). Hence, inter-luminal information is transmitted to the Atg1–Atg13 main switch through the vacuolar membrane via a proper level of Tag1. One reasonable possibility is that Tag1 acts as a sensor of autophagic degradation products including amino acids. We tried to pursue the relationship between the amino acid pool and Tag1-mediated autophagy termination using a mutant of the Atg22 amino acid permease mutant; however, this approach revealed no relationship (data not shown). It would also be interesting to investigate whether the conformation of Tag1 is affected by amino acid concentrations *in vitro*.

Our study provides an avenue for exploring the mechanism by which autophagy is terminated, which in turn determines the ultimate destiny of a cell – survival or autophagic cell death. We have investigated whether the Δ*tag1* mutation affected survival rates under nitrogen starvation, but did not observe a significant phenotype (data not shown). We may still be missing some important piece, such as a back-up system, that would enable us to fully understand the significance of autophagy termination. Nevertheless, this and subsequent studies will facilitate the development of autophagy-related applications for treatment of cancer and neuronal diseases.

MATERIALS AND METHODS

Yeast culture conditions

Yeast cells were grown in YPD [1% yeast extract (BD Biosciences, Franklin Lakes, NJ, USA), 2% peptone (BD Biosciences), 2% glucose (Wako, Osaka, Japan)] or SCD [0.17% yeast nitrogen base without amino acids and ammonium sulfate (BD Biosciences), 0.5% $(NH_4)_2SO_4$ (Nacalai Tesque, Kyoto, Japan], 0.5% casamino acids (BD Biosciences), 2% glucose]. For the starvation condition, the cells were cultured in SD-N buffered with MES (0.17% yeast nitrogen base without amino acids and ammonium sulfate (BD Biosciences), 50 mM MES-NaOH pH 6.2 (Wako), 2% glucose]. Cycloheximide (Wako), rapamycin (LC laboratories, Woburn, Massachusetts) and PMSF (Nacalai) were added to the media at final concentrations of 50 µM, 200 ng/ml and 1 mM, respectively.

Yeast strains and plasmid construction

Yeast strains, plasmids and primers used in this study are listed in Tables S2, S3 and S4, respectively. Gene deletion and tagging were performed using PCR-based methods as previously reported (Janke et al., 2004; Longtine et al., 1998; Nakatogawa et al., 2012a). To make the multiple PP2C deletion

mutant, we used the CRISPR-Cas9 method as previously described (Laughery et al., 2015) with slight modifications. Cells were co-transformed with Cas9 and the gRNA expression plasmid, and the 80-mer single-stranded oligonuclotide DNA as a donor for homologous recombination. Plasmids were cloned using the NEBuilder kit (NEB, E2621) and Gibson assembly (Gibson, 2011). To obtain the linearized vector backbone, pRS series vector (Sikorski and Hieter, 1989) was amplified by inverse PCR. Each insert fragment was amplified by PCR with an 18–20-base tail sequence overlapping each end of the vector backbone. After gel extraction, insert and vector DNA fragments were mixed with 2× NEBuilder HiFi DNA Assembly Master Mix (NEB, E2621) or 2× GA premix [320 µl of 5× ISO buffer, 0.64 µl of 10 U/µl T5 exonuclease (NEB, M0363), 5 µl of 2 U/µl Phusion polymerase (NEB, M0530), 40 µl of 40 Taq DNA ligase (NEB, M208), and 435 µl dH_2O] and incubated for 1 h at 50°C. The mixture was subsequently transformed in *E. coli*. MNY069, which contains a genomic integration of GFP–Tag1, was generated as follows. The hygromycin resistance marker gene (*hphNT1*) cassette from pFA6a-NT1, proTag1, and GFP DNA fragments were amplified. These three DNA fragments were connected by PCR to generate hphNT1-proTag1-GFP, and this fragment was then integrated into the Tag1 N-terminus. The proTag1-GFP-Tag1-Tag1 terminator fragment was amplified from MNY069 genomic DNA using primers oSK1492 and oSK1127, and the pRS316 vector backbone was amplified by inverse PCR with oSK1063 and 1064; the resultant amplicons were connected using the NEBuilder kit (NEB, E2621) to generate pSK402.

Microscopy

Cells were collected by centrifugation (600 ***g***, 2 min) and observed using a Leica AF6500 fluorescence imaging system mounted on a DIM6000 B microscope (HCX PL APO 100×/1.40-0.70 oil-immersion objective lens, xenon lamp; Leica Microsystems) under the control of the LAS-AF software (Leica Microsystems). Cells expressing Atg13–mCherry were observed using an Olympus SpinSR10 imaging system [UPLS APO 100× oil immersion objective lens, and spinning disk unit (CSU-W1, Yokokawa)]. For FM4-64 staining, 1–2 OD units of cells were collected, resuspended in 100 µl SCD containing 1.64 µM FM4-64 (Sigma-Aldrich), and cultured for 1 h at 30°C. After washing, cells were resuspended in 1 ml SCD for 30 min at 30°C.

Antibodies

Anti-Atg proteins used in this study were kind gifts from Dr Ohsumi Yoshinori (Tokyo Institute of Technology, Tokyo, Japan) and are described in the indicated publications: anti-Atg1 (1:2000; Matsuura et al., 1997); anti-Atg2 (1:5000; Shintani et al., 2001); anti-Atg3 (1:2500; Ichimura et al., 2000); anti-Atg4 (1:2000; Nakatogawa et al., 2012a); anti-Atg7 (1:500; Noda et al., 2011); anti-Atg8 (1:1000; Kirisako et al., 2000); anti-Atg9 (1:1000; Noda et al., 2000); anti-Atg12 (1:1000; Kuma et al., 2002); anti-Atg13 (1:200), anti-Atg13 S379 (1:5000), and S428/S429 (1:5000) (Fujioka et al., 2014; Yamamoto et al., 2016); and anti-Atg18 (1:2000), anti-Vps15 (1:1000) and Vps34 (1:2000) (Kihara et al., 2001). Anti-PGK (1:10,000; Life Technologies, 459250), anti-HA (1:1000; Roche, 3F10), anti-Protein A (1:5000; Sigma Aldrich, P3775) and anti-FLAG (1:1000; Sigma Aldrich, M2) antibodies were used for western blotting. Anti-Sch9 (1:3000) and anti–Sch9 phospho-T717 polyclonal antibodies (1:3000) were generated by immunizing rabbits with the synthesized phosphorylated peptide fragment of Sch9. Secondary antibodies for anti-mouse IgG (1:5000; Southern Biotech, 1031-05), anti-rabbit IgG (1:5000; Cell Signaling Technology, 7074) and anti-goat IgG (1:5000; Cell Signaling Technology, 7077) were used.

Genome-wide screening of ALP assay

The yeast knockout library and the DAmP essential gene knockdown library harboring the Pho8Δ60 allele, constructed by the SGA method, were prepared as described previously (Kira et al., 2014). Cells spots were plated on YPD in rectangular OmniTrays (242811, Thermo Fisher Scientific, Waltham, MA, USA), cultured for 24 h at 30°C, cultured for 0, 4 or 24 h in SD-N with MES, and subjected directly to the ALP assay. Assays were performed as previously reported (Kira et al., 2014).

Conventional ALP assays for autophagy measurement

ALP assays for autophagy activity measurements were performed as previously reported (Noda and Klionsky, 2008).

qPCR analysis

Ten OD units of cells were suspended in 400 µl of TES buffer (10 mM Tris-HCl pH 7.5, 0.5% SDS and 10 mM EDTA) and lysed with zirconia beads (ϕ=0.6 mm, Biomedical Science) by vortexing vigorously for 10 min. RNA purification and cDNA synthesis were performed using the RNeasy mini kit (Qiagen) and Script cDNA Synthesis kit (Bio-Rad), respectively. mRNA level (normalized against *ACT1*) was measured by QuantiTect SYBR Green PCR (Qiagen) on a StepOne Plus Realtime PCR system (Life Technologies) using the ΔΔCt method.

Western blotting

For sample preparation, 1–2 OD units of cells were collected and resuspended in 200 µl of 0.3 M NaOH for 10 min at room temperature. Cells were resuspended in 100 µl of SDS-PAGE sample buffer and boiled for 5 min. For sample preparation for western blotting with antibodies against Atg9, Atg13, Atg13 S379, Sch9, Sch9 T717 and Protein A, 2–3 OD units of cells were transferred to a 1.5-ml screw cap tube to which trichloroacetic acid (Wako) was added at a final concentration of 6%, and incubated on ice for at least 20 min. Cells were washed with 700 µl of ice-cold acetone, dried, resuspended in 200 µl of urea buffer [50 mM Tris-HCl pH 7.5, 6 M urea, 5 mM EDTA, 1% SDS, 1 mM PMSF, 1× Complete (Roche), 1× PhosSTOP (Roche)] and 400 µl of zirconia silica beads (ϕ=0.6 mm, Biomedical Science, Tokyo), and lysed with FastPrep (MP-BioMedicals). 2-mercaptoethanol (2 µl; Wako) and a tip of Bromophenol Blue were added, and the samples were incubated for 5 min at 65°C. For EndoH treatment, cells were lysed in a bead beater; the crude lysates were treated with or without 500 U of EndoH (NEB, P0702) at 37°C for 3 h, and then subjected to western blot analysis.

TAP pulldown

Fifty OD units of cells expressing TAP or 4×Protein A-tagged proteins were collected in each tube, resuspended in 400 µl lysis buffer (50 mM Tris-HCl pH 8.0, 150 mM NaCl, 1 mM EDTA, 10% glycerol, 1 mM PMSF, 1× Complete and 1× PhosSTOP) with 400 µl of zirconia silica beads, and lysed with FastPrep. Triton X-100 was added to a final concentration of 1%, and the samples were rotated for 10 min at 4°C. After cell debris was eliminated by centrifugation (20,000 ***g***, 10 min, 4°C), IgG Sepharose 6 Fast Flow (GE) or IgG Dynabeads were added, and the samples were rotated for 2 h at 4°C. Samples were washed three times with the lysis buffer and subjected to downstream analysis.

In vitro kinase assays

For radioisotope labeling, Atg13–TAP proteins were immunopurified from *atg1*Δ cells. After intensive washing steps of the IgG Dynabeads, bound proteins were used as substrates for *in vitro* phosphorylation experiments. Atg1–3×FLAG (wt) and $Atg1^{D211A}$1–3×FLAG (kd) were prepared from yeast cells grown in the presence of rapamycin. Harvested cells were resuspended in lysis buffer supplied with 1 mM PMSF, Complete EDTA-free protease inhibitor cocktail (Roche), 50 mM NaF, 2 mM Na_3VO_4, 10 mM $Na_4P_2O_7$, and 60 mM β-glycerophosphate. Atg1–3×FLAG (wt) and $Atg1^{D211A}$–3×FLAG (kd) were precipitated with anti-FLAG M2 affinity gel (Sigma-Aldrich). The beads were washed three times, followed by elution of the bound proteins by 3×FLAG peptide (Sigma, 1 mg/ml final concentration) in kinase buffer (50 mM Tris-HCl pH 7.5, 75 mM NaCl, 5% glycerol, 10 mM $MgCl_2$ and 1 mM DTT). Reactions were incubated at 30°C for 30 min in kinase buffer with 10 µM ATP and 10 µCi γ-[^{32}P]ATP. The reactions were terminated in HU buffer (50 mM Tris-HCl pH 7.5, 6 M urea, 5 mM EDTA and 1% SDS) by heating for 15 min at 65°C, and proteins were resolved by SDS-PAGE and analyzed on a phosphorimager (FLA-300; Fujifilm).

For detection of Atg13 phosphorylation by western blotting, Atg13–GFP proteins were immunopurified from *atg1*Δ cells using GFP Trap Magnetic agarose (Chromotek). The Atg13-bound beads were incubated with the

Atg1–3×FLAG described in the previous section at 30°C for 1 h in kinase buffer containing 1 mM ATP. Reactions were terminated by addition of SDS-PAGE sample buffer and incubation for 10 min at 95°C, and the samples were subjected to western blot analysis.

LC-MS/MS analysis

Atg13-TAP proteins were immunopurified with the IgG sepharose 6 Fast Flow from WT or Δ*atg1* cells starved for 0 and 24 h. Bound proteins were eluted with Laemmli buffer, followed by SDS-PAGE. The proteins were excised from each gel, destained and digested in the gels with 12.5 ng/µl trypsin (Wako) in 50 mM ammonium bicarbonate overnight at 37°C. The phosphopeptides were enriched with Titansphere Phos-Tio kit (GL Sciences) and desalted with Empore Disk SDB-XC (GL Sciences). Nanoscale liquid chromatography coupled to tandem mass spectrometry (nanoLC-MS/MS) analysis was conducted using a Q Exacitve hybrid quadrupole-orbitrap mass spectrometer (Thermo Fisher Scientific), with Xcalibur software, and coupled to an EASY-nLC 1000 (Thermo Fisher Scientific). The data were processed, searched and LFQ-quantified using the Proteome Discoverer (version 2.4.0.305, Thermo Fisher Scientific), employing the *S. cerevisiae* UniProt database (version Feb. 21, 2016) containing 6749 entries. The search parameters were as follows: trypsin digestion with two missed cleavage permitted; variable modifications, protein N-terminal acetylation, oxidation of methionine, propionamidation of cysteine and phosphorylation of serine, threonine and tyrosine; peptide charge (2+, 3+ and 4+); peptide mass tolerance for MS data, ±10 ppm; and fragment mass tolerance, ±0.02 Da.

Acknowledgements

We are grateful to Dr Hayashi Yamamoto, Dr Sho Suzuki, and Dr Yoshinori Ohsumi for kind gifts of antibodies and plasmids, as well as valuable experimental advice. We also thank Dr Kuninori Suzuki for providing plasmids.

Competing interests

The authors declare no competing or financial interests.

Author contributions

Conceptualization: S.K., T.N.; Methodology: Y.A.; Validation: Y.A.; Formal analysis: S.K.; Investigation: S.K., M.N., Y.O., A.M.; Resources: Y.A., T.Y.; Data curation: S.K., Y.O.; Writing - original draft: S.K.; Writing - review & editing: T.N.; Visualization: S.K.; Supervision: T.N.; Project administration: T.N.; Funding acquisition: T.N.

Funding

This research was supported by the Japan Society for the Promotion of Science (grant number 16K18539 to S.K.) and the Ministry of Education, Culture, Sports, Science and Technology of Japan (grant numbers 16H01202 and 20H05326 to T.N.).

Supplementary information

Supplementary information available online at
https://jcs.biologists.org/lookup/doi/10.1242/jcs.253682.supplemental

References

Albuquerque, C. P., Smolka, M. B., Payne, S. H., Bafna, V., Eng, J. and Zhou, H. (2008). A multidimensional chromatography technology for in-depth phosphoproteome analysis. *Mol. Cell. Proteomics* **7**, 1389-1396. doi:10.1074/mcp.M700468-MCP200

Antonioli, M., Albiero, F., Nazio, F., Vescovo, T., Perdomo, A. B., Corazzari, M., Marsella, C., Piselli, P., Gretzmeier, C., Dengjel, J. et al. (2014). AMBRA1 interplay with cullin E3 ubiquitin ligases regulates autophagy dynamics. *Dev. Cell* **31**, 734-746. doi:10.1016/j.devcel.2014.11.013

Araki, Y., Kira, S. and Noda, T. (2017). Quantitative assay of macroautophagy using Pho8Δ60 assay and GFP-cleavage assay in yeast. *Methods Enzymol.* **588**, 307-321. doi:10.1016/bs.mie.2016.10.027

Cowles, C. R., Odorizzi, G., Payne, G. S. and Emr, S. D. (1997). The AP-3 adaptor complex is essential for cargo-selective transport to the yeast vacuole. *Cell* **91**, 109-118. doi:10.1016/s0092-8674(01)80013-1

Darsow, T., Burd, C. G. and Emr, S. D. (1998). Acidic di-leucine motif essential for AP-3-dependent sorting and restriction of the functional specificity of the Vam3p vacuolar t-SNARE. *J. Cell Biol.* **142**, 913-922. doi:10.1083/jcb.142.4.913

Epple, U. D., Suriapranata, I., Eskelinen, E.-L. and Thumm, M. (2001). Aut5/Cvt17p, a putative lipase essential for disintegration of autophagic bodies inside the vacuole. *J. Bacteriol.* **183**, 5942-5955. doi:10.1128/JB.183.20.5942-5955.2001

Fujioka, Y., Suzuki, S. W., Yamamoto, H., Kondo-Kakuta, C., Kimura, Y., Hirano, H., Akada, R., Inagaki, F., Ohsumi, Y. and Noda, N. N. (2014). Structural basis of starvation-induced assembly of the autophagy initiation complex. *Nat. Struct. Mol. Biol.* **21**, 513-521. doi:10.1038/nsmb.2822

Fujioka, Y., Alam, J. M., Noshiro, D., Mouri, K., Ando, T., Okada, Y., May, A. I., Knorr, R. L., Suzuki, K., Ohsumi, Y. et al. (2020). Phase separation organizes the site of autophagosome formation. *Nature* **578**, 301-305. doi:10.1038/s41586-020-1977-6

Gibson, D. G. (2011). Enzymatic assembly of overlapping DNA fragments. *Methods Enzymol.* **498**, 349-361. doi:10.1016/B978-0-12-385120-8.00015-2

Gnanasundram, S. V. and Koš, M. (2015). Fast protein-depletion system utilizing tetracycline repressible promoter and N-end rule in yeast. *Mol. Biol. Cell* **26**, 762-768. doi:10.1091/mbc.E14-07-1186

Hecht, K. A., Donnell, A. F. O. and Brodsky, J. L. (2014). The proteolytic landscape of the yeast vacuole. *Cellular Logistics* **4**, e28023. doi:10.4161/cl.28023

Holt, L. J., Tuch, B. B., Villen, J., Johnson, A. D., Gygi, S. P. and Morgan, D. O. (2009). Global analysis of Cdk1 substrate phosphorylation sites provides insights into evolution. *Science* **325**, 1682-1686. doi:10.1126/science.1172867

Huang, H., Kawamata, T., Horie, T., Tsugawa, H., Nakayama, Y., Ohsumi, Y. and Fukusaki, E. (2015). Bulk RNA degradation by nitrogen starvation-induced autophagy in yeast. *EMBO J.* **34**, 154-168. doi:10.15252/embj.201489083

Ichimura, Y., Kirisako, T., Takao, T., Satomi, Y., Shimonishi, Y., Ishihara, N., Mizushima, N., Tanida, I., Kominami, E., Ohsumi, M. et al. (2000). A ubiquitin-like system mediates protein lipidation. *Nature* **408**, 488-492. doi:10.1038/35044114

Janke, C., Magiera, M. M., Rathfelder, N., Taxis, C., Reber, S., Maekawa, H., Moreno-Borchart, A., Doenges, G., Schwob, E., Schiebel, E. et al. (2004). A versatile toolbox for PCR-based tagging of yeast genes: new fluorescent proteins, more markers and promoter substitution cassettes. *Yeast* **21**, 947-962. doi:10.1002/yea.1142

Kamada, Y., Funakoshi, T., Shintani, T., Nagano, K., Ohsumi, M. and Ohsumi, Y. (2000). Tor-mediated induction of autophagy via an Apg1 protein kinase complex. *J. Cell Biol.* **150**, 1507-1513. doi:10.1083/jcb.150.6.1507

Kamada, Y., Yoshino, K. I., Kondo, C., Kawamata, T., Oshiro, N., Yonezawa, K. and Ohsumi, Y. (2009). Tor directly controls the Atg1 kinase complex to regulate autophagy. *Mol. Cell. Biol.* **30**, 1049-1058. doi:10.1128/MCB.01344-09

Katzmann, D. J., Babst, M. and Emr, S. D. (2001). Ubiquitin-dependent sorting into the multivesicular body pathway requires the function of a conserved endosomal protein sorting complex, ESCRT-I. *Cell* **106**, 145-155. doi:10.1016/S0092-8674(01)00434-2

Kawamata, T., Kamada, Y., Kabeya, Y., Sekito, T. and Ohsumi, Y. (2008). Organization of the pre-autophagosomal structure responsible for autophagosome formation. *Mol. Biol. Cell* **19**, 2039-2050. doi:10.1091/mbc.e07-10-1048

Kihara, A., Noda, T., Ishihara, N. and Ohsumi, Y. (2001). Two distinct Vps34 phosphatidylinositol 3-kinase complexes function in autophagy and carboxypeptidase Y sorting in Saccharomyces cerevisiae. *J. Cell Biol.* **152**, 519-530. doi:10.1083/jcb.152.3.519

Kim, A. and Cunningham, K. W. (2015). A LAPF/phafin1-like protein regulates TORC1 and lysosomal membrane permeabilization in response to endoplasmic reticulum membrane stress. *Mol. Biol. Cell* **26**, 4631-4645. doi:10.1091/mbc.E15-08-0581

Kira, S., Tabata, K., Shirahama-Noda, K., Nozoe, A., Yoshimori, T. and Noda, T. (2014). Reciprocal conversion of Gtr1 and Gtr2 nucleotide-binding states by Npr2-Npr3 inactivates TORC1 and induces autophagy. *Autophagy* **10**, 1565-1578. doi:10.4161/auto.29397

Kira, S., Kumano, Y., Ukai, H., Takeda, E., Matsuura, A. and Noda, T. (2016). Dynamic relocation of the TORC1-Gtr1/2-Ego1/2/3 complex is regulated by Gtr1 and Gtr2. *Mol. Biol. Cell* **27**, 382-396. doi:10.1091/mbc.e15-07-0470

Kirisako, T., Ichimura, Y., Okada, H., Kabeya, Y., Mizushima, N., Yoshimori, T., Ohsumi, M., Takao, T., Noda, T. and Ohsumi, Y. (2000). The reversible modification regulates the membrane-binding state of Apg8/Aut7 essential for autophagy and the cytoplasm to vacuole targeting pathway. *J. Cell Biol.* **151**, 263-276. doi:10.1083/jcb.151.2.263

Klionsky, D. J. and Emr, S. D. (1989). Membrane protein sorting: biosynthesis, transport and processing of yeast vacuolar alkaline phosphatase. *EMBO J.* **8**, 2241-2250. doi:10.1002/j.1460-2075.1989.tb08348.x

Kraft, C., Kijanska, M., Kalie, E., Siergiejuk, E., Lee, S. S., Semplicio, G., Stoffel, I., Brezovich, A., Verma, M., Hansmann, I. et al. (2012). Binding of the Atg1/ULK1 kinase to the ubiquitin-like protein Atg8 regulates autophagy. *EMBO J.* **31**, 3691-3703. doi:10.1038/emboj.2012.225

Kroemer, G. and Levine, B. (2008). Autophagic cell death: the story of a misnomer. *Nat. Rev. Mol. Cell Biol.* **9**, 1004-1010. doi:10.1038/nrm2529

Kuma, A., Mizushima, N., Ishihara, N. and Ohsumi, Y. (2002). Formation of the ~350-kDa Apg12-Apg5 Apg16 multimeric complex, mediated by Apg16 oligomerization, is essential for autophagy in yeast. *J. Biol. Chem.* **277**, 18619-18625. doi:10.1074/jbc.M111889200

Laughery, M. F., Hunter, T., Brown, A., Hoopes, J., Ostbye, T., Shumaker, T. and Wyrick, J. J. (2015). New vectors for simple and streamlined CRISPR-Cas9 genome editing in Saccharomyces cerevisiae. *Yeast* **32**, 711-720. doi:10.1002/yea.3098

Liu, C.-C., Lin, Y.-C., Chen, Y.-H., Chen, C.-M., Pang, L.-Y., Chen, H.-A., Wu, P.-R., Lin, M.-Y., Jiang, S.-T., Tsai, T.-F. et al. (2016). Cul3-KLHL20 ubiquitin ligase governs the turnover of ULK1 and VPS34 complexes to control autophagy termination. *Mol. Cell* **61**, 84-97. doi:10.1016/j.molcel.2015.11.001

Longtine, M. S., McKenzie, A. R., Demarini, D. J., Shah, N. G., Wach, A., Brachat, A., Philippsen, P. and Pringle, J. R. (1998). Additional modules for versatile and economical PCR-based gene deletion and modification in Saccharomyces cerevisiae. *Yeast* **14**, 953-961. doi:10.1002/(SICI)1097-0061(199807)14:10<953::AID-YEA293>3.0.CO;2-U

Mao, K., Chew, L. H., Inoue-Aono, Y., Cheong, H., Nair, U., Popelka, H., Yip, C. K. and Klionsky, D. J. (2013). Atg29 phosphorylation regulates coordination of the Atg17-Atg31-Atg29 complex with the Atg11 scaffold during autophagy initiation. *Proc. Natl. Acad. Sci. USA* **110**, E2875-E2884. doi:10.1073/pnas.1300064110

Matsuura, A., Tsukada, M., Wada, Y. and Ohsumi, Y. (1997). Apg1p, a novel protein kinase required for the autophagic process in Saccharomyces cerevisiae. *Gene* **192**, 245-250. doi:10.1016/S0378-1119(97)00084-X

McIsaac, R. S., Oakes, B. L., Wang, X., Dummit, K. A., Botstein, D. and Noyes, M. B. (2013). Synthetic gene expression perturbation systems with rapid, tunable, single-gene specificity in yeast. *Nucleic Acids Res.* **41**, e57. doi:10.1093/nar/gks1313

Memisoglu, G., Eapen, V. V., Yang, Y., Klionsky, D. J. and Haber, J. E. (2019). PP2C phosphatases promote autophagy by dephosphorylation of the Atg1 complex. *Proc. Natl. Acad. Sci. USA* **116**, 1613-1620. doi:10.1073/pnas.1817078116

Michel, A. H., Hatakeyama, R., Kimmig, P., Arter, M., Peter, M., Matos, J., De Virgilio, C. and Kornmann, B. (2017). Functional mapping of yeast genomes by saturated transposition. *Elife* **6**, 23570. doi:10.7554/eLife.23570

Mizushima, N. and Komatsu, M. (2011). Autophagy: renovation of cells and tissues. *Cell* **147**, 728-741. doi:10.1016/j.cell.2011.10.026

Nakatogawa, H., Ishii, J., Asai, E. and Ohsumi, Y. (2012a). Atg4 recycles inappropriately lipidated Atg8 to promote autophagosome biogenesis. *Autophagy* **8**, 177-186. doi:10.4161/auto.8.2.18373

Nakatogawa, H., Ohbayashi, S., Sakoh-Nakatogawa, M., Kakuta, S., Suzuki, S. W., Kirisako, H., Kondo-Kakuta, C., Noda, N. N., Yamamoto, H. and Ohsumi, Y. (2012b). The autophagy-related protein kinase Atg1 interacts with the ubiquitin-like protein Atg8 via the Atg8 family interacting motif to facilitate autophagosome formation. *J. Biol. Chem.* **287**, 28503-28507. doi:10.1074/jbc.C112.387514

Nazio, F., Carinci, M., Valacca, C., Bielli, P., Strappazzon, F., Antonioli, M., Ciccosanti, F., Rodolfo, C., Campello, S., Fimia, G. M. et al. (2016). Fine-tuning of ULK1 mRNA and protein levels is required for autophagy oscillation. *J. Cell Biol.* **215**, 841-856. doi:10.1083/jcb.201605089

Noda, T. (2017). Regulation of Autophagy through TORC1 and mTORC1. *Biomolecules* **7**, 52. doi:10.3390/biom7030052

Noda, T. and Klionsky, D. J. (2008). The quantitative Pho8Delta60 assay of nonspecific autophagy. *Methods Enzymol.* **451**, 33-42. doi:10.1016/S0076-6879(08)03203-5

Noda, T., Matsuura, A., Wada, Y. and Ohsumi, Y. (1995). Novel system for monitoring autophagy in the yeast Saccharomyces cerevisiae. *Biochem. Biophys. Res. Commun.* **210**, 126-132. doi:10.1006/bbrc.1995.1636

Noda, T., Kim, J., Huang, W. P., Baba, M., Tokunaga, C., Ohsumi, Y. and Klionsky, D. J. (2000). Apg9p/Cvt7p is an integral membrane protein required for transport vesicle formation in the Cvt and autophagy pathways. *J. Cell Biol.* **148**, 465-480. doi:10.1083/jcb.148.3.465

Noda, N. N., Satoo, K., Fujioka, Y., Kumeta, H., Ogura, K., Nakatogawa, H., Ohsumi, Y. and Inagaki, F. (2011). Structural basis of atg8 activation by a homodimeric e1, atg7. *Mol. Cell.* **44**, 462-475. doi:10.1016/j.molcel.2011.08.035

Odorizzi, G., Babst, M. and Emr, S. D. (1998). Fab1p PtdIns(3)P 5-kinase function essential for protein sorting in the multivesicular body. *Cell* **95**, 847-858. doi:10.1016/S0092-8674(00)81707-9

Oku, M., Maeda, Y., Kagohashi, Y., Kondo, T., Yamada, M., Fujimoto, T. and Sakai, Y. (2017). Evidence for ESCRT- and clathrin-dependent microautophagy. *J. Cell Biol.* **216**, 3263-3274. doi:10.1083/jcb.201611029

Papinski, D., Schuschnig, M., Reiter, W., Wilhelm, L., Barnes, C. A., Maiolica, A., Hansmann, I., Pfaffenwimmer, T., Kijanska, M., Stoffel, I. et al. (2014). Early steps in autophagy depend on direct phosphorylation of Atg9 by the Atg1 kinase. *Mol. Cell* **53**, 471-483. doi:10.1016/j.molcel.2013.12.011

Péli-Gulli, M.-P., Sardu, A., Panchaud, N., Raucci, S. and De Virgilio, C. (2015). Amino acids stimulate TORC1 through Lst4-Lst7, a GTPase-activating protein complex for the rag family GTPase Gtr2. *Cell Rep* **13**, 1-7. doi:10.1016/j.celrep.2015.08.059

Petit, C. S., Roczniak-Ferguson, A. and Ferguson, S. M. (2013). Recruitment of folliculin to lysosomes supports the amino acid-dependent activation of Rag GTPases. *J. Cell Biol.* **202**, 1107-1122. doi:10.1083/jcb.201307084

Reggiori, F. and Klionsky, D. J. (2013). Autophagic processes in yeast: mechanism, machinery and regulation. *Genetics* **194**, 341-361. doi:10.1534/genetics.112.149013

Schuldiner, M., Collins, S. R., Thompson, N. J., Denic, V., Bhamidipati, A., Punna, T., Ihmels, J., Andrews, B., Boone, C., Greenblatt, J. F. et al. (2005). Exploration of the function and organization of the yeast early secretory pathway through an epistatic miniarray profile. *Cell* **123**, 507-519. doi:10.1016/j.cell.2005.08.031

Shin, C. S. and Huh, W. K. (2011). Bidirectional regulation between TORC1 and autophagy in Saccharomyces cerevisiae. *Autophagy* **7**, 854-862. doi:10.4161/auto.7.8.15696

Shintani, T. and Klionsky, D. J. (2004). Cargo proteins facilitate the formation of transport vesicles in the cytoplasm to vacuole targeting pathway. *J. Biol. Chem.* **279**, 29889-29894. doi:10.1074/jbc.M404399200

Shintani, T., Suzuki, K., Kamada, Y., Noda, T. and Ohsumi, Y. (2001). Apg2p functions in autophagosome formation on the perivacuolar structure. *J. Biol. Chem.* **276**, 30452-30460. doi:10.1074/jbc.M102346200

Shirahama-Noda, K., Kira, S., Yoshimori, T. and Noda, T. (2013). TRAPPIII is responsible for vesicular transport from early endosomes to Golgi, facilitating Atg9 cycling in autophagy. *J. Cell Sci.* **126**, 4963-4973. doi:10.1242/jcs.131318

Sikorski, R. S. and Hieter, P. (1989). A system of shuttle vectors and yeast host strains designed for efficient manipulation of DNA in Saccharomyces cerevisiae. *Genetics* **122**, 19-27. doi:10.1093/genetics/122.1.19

Swaney, D. L., Beltrao, P., Starita, L., Guo, A., Rush, J., Fields, S., Krogan, N. J. and Villen, J. (2013). Global analysis of phosphorylation and ubiquitylation cross-talk in protein degradation. *Nat. Methods* **10**, 676-682. doi:10.1038/nmeth.2519

Takeshige, K., Baba, M., Tsuboi, S., Noda, T. and Ohsumi, Y. (1992). Autophagy in yeast demonstrated with proteinase-deficient mutants and conditions for its induction. *J. Cell Biol.* **119**, 301-311. doi:10.1083/jcb.119.2.301

Tanigawa, M. and Maeda, T. (2017). An In Vitro TORC1 kinase assay that recapitulates the Gtr-independent glutamine-responsive TORC1 activation mechanism on yeast vacuoles. *Mol. Cell. Biol.* **37**, e00075-e00017. doi:10.1128/MCB.00075-17

Tsun, Z.-Y., Bar-Peled, L., Chantranupong, L., Zoncu, R., Wang, T., Kim, C., Spooner, E. and Sabatini, D. M. (2013). The folliculin tumor suppressor is a GAP for the RagC/D GTPases that signal amino acid levels to mTORC1. *Mol. Cell* **52**, 495-505. doi:10.1016/j.molcel.2013.09.016

Ukai, H., Araki, Y., Kira, S., Oikawa, Y., May, A. I. and Noda, T. (2018). Gtr/Ego-independent TORC1 activation is achieved through a glutamine-sensitive interaction with Pib2 on the vacuolar membrane. *PLoS Genet.* **14**, e1007334. doi:10.1371/journal.pgen.1007334

Umekawa, M. and Klionsky, D. J. (2012). Ksp1 kinase regulates autophagy via the target of rapamycin complex 1 (TORC1) pathway. *J. Biol. Chem.* **287**, 16300-16310. doi:10.1074/jbc.M112.344952

Urban, J., Soulard, A., Huber, A., Lippman, S., Mukhopadhyay, D., Deloche, O., Wanke, V., Anrather, D., Ammerer, G., Riezman, H. et al. (2007). Sch9 is a major target of TORC1 in Saccharomyces cerevisiae. *Mol. Cell* **26**, 663-674. doi:10.1016/j.molcel.2007.04.020

Varlakhanova, N. V., Mihalevic, M. J., Bernstein, K. A. and Ford, M. G. J. (2017). Pib2 and the EGO complex are both required for activation of TORC1. *J. Cell Sci.* **130**, 3878-3890. doi:10.1242/jcs.207910

Wiederhold, E., Gandhi, T., Permentier, H. P., Breitling, R., Poolman, B. and Slotboom, D. J. (2009). The yeast vacuolar membrane proteome. *Mol. Cell. Proteomics* **8**, 380-392. doi:10.1074/mcp.M800372-MCP200

Yamamoto, H., Fujioka, Y., Suzuki, S. W., Noshiro, D., Suzuki, H., Kondo-Kakuta, C., Kimura, Y., Hirano, H., Ando, T., Noda, N. N. et al. (2016). The intrinsically disordered protein Atg13 mediates supramolecular assembly of autophagy initiation complexes. *Dev. Cell* **38**, 86-99. doi:10.1016/j.devcel.2016.06.015

Yu, L., McPhee, C. K., Zheng, L., Mardones, G. A., Rong, Y., Peng, J., Mi, N., Zhao, Y., Liu, Z., Wan, F. et al. (2010). Termination of autophagy and reformation of lysosomes regulated by mTOR. *Nature* **465**, 942-946. doi:10.1038/nature09076

Zhu, L., Jorgensen, J. R., Li, M., Chuang, Y. S. and Emr, S. D. (2017). ESCRTs function directly on the lysosome membrane to downregulate ubiquitinated lysosomal membrane proteins. *Elife* **6**, 26403. doi:10.7554/eLife.26403